

Supplementary Material for:

Abnormal Brain Response to Cholinergic Challenge in Chronic Encephalopathy from the 1991 Gulf War

Robert W. Haley, Jeffrey S. Spence, Patrick S. Carmack,
Richard F. Gunst, William R. Schucany, Frederick Petty, Michael D. Devous, Sr.,
Frederick J. Bonte, Madhukar H. Trivedi

S1. Supplementary Statistical Methods for Spatial Modeling

To test for differences in nrCBF among the four clinical groups that were expected to be subtle and beyond the resolution of standard brain imaging analytic approaches such as SPM, we developed and applied a novel statistical approach capable of detecting more subtle group differences. We briefly summarize the approach here and refer the interested reader to the full statistical description (**Spence et al., 2007**).

A troublesome problem in the analysis of brain imaging data that has never been satisfactorily addressed is the correlation among nearby voxels, which results from limitations in the resolution of brain scanning devices (e.g., filtering in image construction) and possibly the functional association of nearby brain cells measured by contiguous voxels. Brain imaging data with substantial intervoxel correlations fail to satisfy the usual independence assumption of statistical linear models that are typically applied to them. Standard methods of brain image analysis generally address this by applying 8-14 mm kernel smoothing and corrected statistical tests based on the expected Euler characteristic in Gaussian random field theory (**Frackowiak et al., 1997**). This approach tends to work satisfactorily in identifying group differences of large magnitude or wide extent that survive smoothing but lacks sensitivity to differences that are smaller in magnitude and/or extent. Since more subtle group differences are expected in neuropsychiatric conditions such as Gulf War syndrome, we developed an alternative analytic approach (**Spence et al., 2007**) based on the extensive body of theory from geostatistical *spatial modeling*, or kriging (**Matheron, 1973; Isaaks and Srivastava, 1989; Cressie, 1993**), not previously applied to testing for group differences in brain imaging.

The basic approach of spatial modeling is to identify the covariance structure of measurements in a three-dimensional dataset by statistically fitting *semivariogram* models to small regions of interest (**Spence et al., 2007**). A semivariogram is a plot of the “variance” or “semivariogram value,” defined as *half the variance of the pairwise intervoxel distances as a function of the distance between the voxels of the pair* (**Supplementary Fig. S1A**). It is used to estimate the three key parameters of the spatial covariance structure, the *nugget*, the *sill* and the *range*. From these, best linear unbiased prediction (BLUP) methods (**Cressie, 1993**) are used to estimate the true mean intensity in small regions of correlated voxels called *blocks*. We found that in the SPECT images from our study the nugget was not significantly different from zero, and the range was between 4 and 7 voxels distance in virtually all deep brain regions regardless of the magnitude of the sill, which varied by subject and structure (**Supplementary Fig. S1B**). Consequently, voxels more than 4-7 voxels apart are free of the effects of correlation among neighboring voxels. Note that this correlation among neighboring voxels is different from the covariance among distant ROIs due to functional associations among brain structures.

In each deep brain structure two or more blocks of contiguous voxels were defined by the investigators with the assistance of an automated semivariogram program so that the geometric centers of adjacent blocks would be no closer than the range of the semivariogram (4-7 voxels

distance), thus ensuring that the block averages would be free of the effects of the intervoxel correlations (Spence et al., 2007). Within this constraint of the semivariogram range condition, the block locations were defined to reflect the known nuclear substructure of the deep brain structures; for example, separate blocks were defined to approximate the corticomедial and basolateral divisions of the amygdala and the seven main nuclei of the thalamus with the larger ones further subdivided (Supplementary Fig. S1C). Deep structures without known nuclear substructure (e.g., putamen, pons) were subdivided into as many blocks as possible that would satisfy the semivariogram range condition. Use of a new affine transformation to map the sets of Talairach coordinates to the MNI152 template in reference to the surfaces of the ventricles rather than the brain surface allowed us to locate deep brain structures, such as the thalamic nuclei, more accurately than previous transformation approaches (Carmack et al., 2004).

Block averages and their variances were calculated and extracted to a dataset to obtain data that satisfy the usual independence assumptions of statistical linear models (Spence et al., 2007). In addition, for each deep brain structure, a weighted *structure average* was calculated from its component block averages using the reciprocals of their prediction variances as weights. These spatial averaging procedures reduced the number of observations in deep brain gray matter structures from the original approximately 17,000 voxels, containing extensive effects of covariance among nearby voxels, to nrCBF averages for each of the 8 deep brain structures and their 39 component blocks in each hemisphere, containing no effects of covariance among nearby voxels. This reduction in the number of observations for analysis substantially reduced the magnitude of the multiple comparisons problem to be corrected for in the analyses and obviated the need for Gaussian kernel smoothing of the data—both sources of severe loss of statistical sensitivity in previous analyses of group effects in brain imaging data.

S2. Structure-Level Differences Among Groups

Whereas in the paper we presented significant group differences found at the block level (*substructure level*), here we present a systematic description of the group differences at the deep gray matter *structure level* (e.g., amygdala, thalamus, pons) for the baseline images from session 1 (Supplementary Table S1) and for the change in nrCBF from session 1 to session 2 (Supplementary Table S2). These findings differ somewhat from those in the paper primarily due to two effects. First, when only one of several blocks in a structure has a significant group difference, the group difference for the structure as a whole may not be significant. Second, when all, or most, of the blocks within a structure are nearly, but not quite, statistically significant, the joint effect of these blocks may make the group difference significant for the structure as a whole. Instances of these effects are indicated by footnotes in the supplementary tables.

S3. Effects of Controlling for Other Possible Confounding Variables and Covariates

One concern of the investigators was that group effects identified in the analysis could have resulted from confounding by pre-existing differences between the symptom complex and control groups or by unequally distributed experimental conditions. To address this, we measured the most likely confounding variables in the following five categories: personal characteristics, diagnosed underlying medical conditions, prescription medications being taken at home before reporting for the study hospitalization, prescription medications continued during hospitalization, and parameters of the physostigmine experiment and SPECT scanning. All medications considered capable of

interfering with the experiment were discontinued at least three half-lives before arriving for the study hospitalization. Despite this, we tested for confounding all medications being taken before arrival because of the possibility that discontinuation of a certain medication might produce a withdrawal effect capable of influencing nrCBF or its response to physostigmine. Since no diagnosis was present in more than 3 subjects and no medications had been taken at home or during the study by more than 6 subjects, we created summary measures of any underlying diagnosis or any prescription medication taken at home or during the study for use in the analyses of confounding. Exceptions to this were diagnoses of alcohol abuse or post-traumatic stress disorder made by a psychiatrist's structured clinical interview for DSM-IV (SCID) examination during our study. Although these two diagnoses were present in only small numbers of subjects, they were analyzed separately because of the interest in them as possible confounders. The group means or percentages on these characteristics are compared in **Supplementary Table S3**.

We tested each characteristic or medication for confounding by introducing it as a single covariate along with its covariate \times structure interaction into a global mixed-effects model of baseline nrCBF (resulting estimates shown in **Fig. 1A** of the paper) and into a global model of change in nrCBF (estimates shown in **Fig. 1B**). To identify the best small subset of covariates, we generated multivariate regression models for each deep brain structure using the ADJRSQ selection option of SAS Proc Reg set to generate the best six-variable models of baseline nrCBF or change in nrCBF. From the lists of best variables we selected the 3 variables that contributed most to the adjusted R^2 of the models across the 16 structures. These, along with their covariate \times structure interactions, were entered into the two mixed-effects models to assess possible multivariate confounding. We considered the sample size of subjects sufficient for testing for potential confounding by each covariate alone and with the best 3 covariates but not to introduce all 17 covariates in the same model.

Compared to the main findings in the model of baseline nrCBF measured at session 1, none of the 17 covariates entered into the model individually reduced the significance of the group main effect or the contrast for symptom complex 2 vs controls (all group effects still had P values ≤ 0.032 and all symptom complex 2 vs control contrasts still had P values ≤ 0.008 ; **Supplementary Table S4A**). When smoking, lefthandedness and psychiatrist's SCID diagnosis of alcohol abuse—the 3 covariates that were jointly most strongly associated with baseline nrCBF—were entered into the model along with their covariate \times structure interactions, both the group main effect and the contrast for symptom complex 2 vs controls remained significant ($P = 0.037$ and $P = 0.0075$, respectively; **Supplementary Table S4B**). Moreover, with the psychiatrist's SCID diagnosis of post-traumatic stress disorder added to the model because of historical concerns about this link, both the group main effect and the contrast for symptom complex 2 vs controls remained significant ($P = 0.032$ and $P = 0.0063$, respectively; data not shown).

Compared to the main findings in the model of the change in nrCBF from session 1 to session 2, none of the 20 covariates entered into the model individually reduced the significance of the group \times structure interaction, the main finding in the change model (all group \times structure interactions still had P value ≤ 0.02 ; **Supplementary Table S5A**). When lefthandedness, daytime mean arterial blood pressure, and body mass index—the 3 covariates that were jointly most strongly associated with the change in nrCBF— were entered into the model along with their covariate \times structure interactions, the group \times structure interaction remained significant ($P = 0.0031$; **Supplementary Table S5B**). Moreover, with the psychiatrist's SCID diagnoses of post-traumatic stress disorder and alcohol abuse added to the model, the group \times structure interaction remained significant ($P = 0.0071$; data not shown).

We measured the following three features of the physostigmine experiment that could have influenced the findings: dose of physostigmine administered in session 2, differences in the dose of

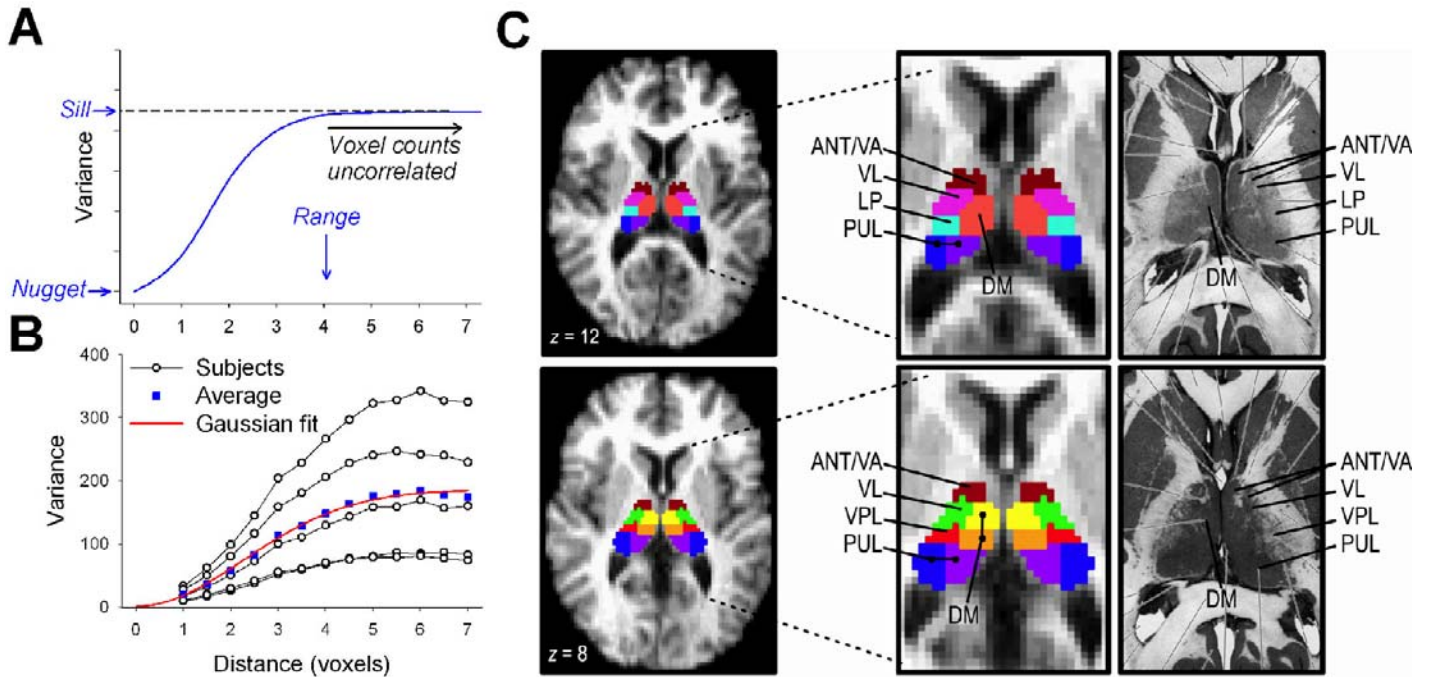
^{99m}Tc -HMPAO administered at session 1 and session 2, and difference in interval from administration of ^{99m}Tc -HMPAO to SPECT scan at the two sessions. Only the physostigmine dose was significantly associated with the change of nrCBF in the univariate analyses (**Supplementary Table S5A**). After controlling for the best combination of 3 other covariates shown in **Supplementary Table S5B**, physostigmine did not remain significant (result not shown). In the global hypothesis test (estimates from which are shown in **Fig. 1B**), controlling for physostigmine dose caused the nonsignificant group main effect and the symptom complex 2 contrasts to become significant; whereas, the originally significant group \times structure interaction remained highly significant (**Supplementary Table S6**).

In the multivariate model of the change in nrCBF, we did not control for baseline nrCBF because controlling for a baseline measure that is part of the response measure introduces a tautological effect into the model that appears to control for baseline effects which are tautological rather than causal. This would often render other independent variables nonsignificant spuriously.

From these analyses we concluded that confounding by the many characteristics and medications analyzed did not influence the findings importantly, although controlling for the physostigmine dose rendered the global hypothesis test more significant.

References

- Carmack, P.S., Spence, J.S., Gunst, R.F., Schucany, W.R., Woodward, W.A., Haley, R.W., 2004. Improved agreement between Talairach and MNI coordinate spaces in deep brain regions. *Neuroimage* 22, 367-371.
- Cressie, N., 1993. *Statistics for Spatial Data*. J. Wiley and Sons, New York
- Frackowiak, R., Friston, K.J., Frith, C.D., Dolan, R., Mazziotta, J.C., 1997. *Human Brain Function*. Academic Press, London
- Hanaway, J., Woolsey, T.A., Gado, M.H., Roberts, Jr. M.P., 1998. *The Brain Atlas: A Visual Guide to the Human Central Nervous System*. Fitzgerald Science Press, Bethesda, Maryland, pp. 92-94.
- Isaaks, E., Srivastava, R., 1989. *An Introduction to Applied Geostatistics*. Oxford University Press, Oxford
- Matheron, G., 1973. The intrinsic rancom functions and their applications. *Journal of Applied Probability* 5, 439-468.
- Spence, J.S., Carmack, P.S., Gunst, R.F., Schucany, W.R., Woodward, W.A., Haley, R.W., 2007. Accounting for spatial dependence in the analysis of SPECT brain imaging data. *JASA Journal of the American Statistical Association* 102, 464-473.



Supplementary Fig. S1. Summary of the statistical procedure for defining statistically independent blocks of correlated voxels for analysis (Spence et al., 2007). (A) Conceptual *semivariogram* plot of the variation in nrCBF among nearby voxels versus the distance between voxels (measured in number of voxels). In all cerebral gray matter regions semivariogram measurements show that nrCBF values of voxels close together vary less (high correlation) and those farther apart (are uncorrelated). This type of statistical correlation, which is related to measurement error, is unrelated to the covariances between distant ROIs that signify functional association. Parameters of a semivariogram plot include the *nugget* (variance among voxels very close together at the sampling point, usually due to measurement, error), the *sill* (variance farther from the sampling point where the normalized voxel counts are uncorrelated); the *range* (distance from the sampling point at which the normalized counts become uncorrelated). (B) Actual semivariogram plots from the baseline SPECT scan of the left thalamus of 5 veterans with Gulf War symptom complex 3. Despite differences in the sill, all had similar ranges between 4 and 5 voxels distance. The range parameter in a given region of a SPECT brain image is well estimated by a Gaussian fit to the semivariograms of multiple subjects. In the analysis of a SPECT experiment, the range parameter is determined in all brain regions by an automated spatial modeling program. In each brain region 2 or more *blocks* of correlated voxels are defined so that the geometric centers of adjacent blocks would be no closer than the value of the range parameter of the region (usually 4-7 voxels distance). Calculating the average intensity over the voxels in a block with best linear unbiased prediction (BLUP) methods yields *block averages*, and their variances, which are statistically uncorrelated nrCBF observations satisfying the assumptions of linear modeling procedures. These observations are extracted to a rectangular datafile for analysis with SAS. This analytic approach exploits the correlation structure of nearby voxels to increase the power to detect group differences in brain imaging experiments. (C) Illustration of the blocks from spatial modeling over the thalamic nuclei in axial cross-sections at the inferior quartile ($Z = 8$) and the superior quartile ($Z = 12$) of the thalamus, compared with nuclear anatomy in labeled cross-sections at comparable levels from a standard brain atlas (Hanaway et al., 1998) (far right). Blocks of correlated voxels were defined so that the centers of adjacent blocks were no nearer than the thalamic semivariogram range value of 4-5 voxels distance to ensure statistical independence. Use of a new affine transformation to map the sets of Talairach coordinates to the MNI152 template in reference to the surfaces of the ventricles rather than the brain surface allowed us to locate deep brain structures, such as the thalamic nuclei, more accurately than previous ones (Carmack et al., 2004). ANT, anterior nucleus; VA, ventral anterior nucleus; VL, ventrolateral nucleus; LP, lateral posterior nucleus; PUL, pulvinar; VPL, ventral posterolateral nucleus; DM, dorsomedial nucleus.

Supplementary Table S1. Mean baseline nrCBF* of the control group and difference between symptom complex groups and the control group at the deep brain structure level

Structure	Effect†	Left				Right			
		mean	std err	t	p	mean	std err	t	p
Amygdala	Con	154.07	3.68			145.01	3.33		
	S1-Con	-1.75	5.98	-0.29	0.771	5.88	8.64	0.68	0.501
	S2-Con	-12.82	5.37	-2.39	0.023 ‡	-5.08	4.91	-1.03	0.308
	S3-Con	6.85	6.05	1.13	0.266	13.94	5.70	2.44	0.020
Caudate head	Con	171.07	3.09			175.64	2.44		
	S1-Con	3.15	7.53	0.42	0.679	0.85	4.86	0.18	0.861
	S2-Con	-11.10	4.23	-2.62	0.013	-11.70	3.86	-3.03	0.005
	S3-Con	-2.07	6.97	-0.30	0.768	-4.03	5.76	-0.70	0.489
Putamen	Con	193.97	2.85			195.60	2.95		
	S1-Con	2.49	6.11	0.41	0.687	8.33	6.33	1.32	0.197
	S2-Con	-14.60	4.68	-3.12	0.004	-13.37	4.34	-3.08	0.004
	S3-Con	1.89	5.96	0.32	0.753	0.83	6.06	0.14	0.892
Globus pallidus	Con	159.54	2.76			158.51	3.28		
	S1-Con	6.66	6.05	1.10	0.279	15.20	7.98	1.90	0.065
	S2-Con	-14.03	4.22	-3.32	0.002	-8.73	5.27	-1.66	0.107
	S3-Con	-7.54	5.82	-1.30	0.204	3.84	7.27	0.53	0.601 §
Thalamus	Con	195.70	3.10			193.81	3.38		
	S1-Con	7.48	7.78	0.96	0.343	8.28	7.51	1.10	0.278
	S2-Con	-16.48	4.98	-3.31	0.002	-12.41	5.05	-2.46	0.019
	S3-Con	0.57	7.79	0.07	0.942	5.51	7.04	0.78	0.439
Hippocampus	Con	152.39	3.37			152.54	3.87		
	S1-Con	-0.22	6.52	-0.03	0.973	1.73	9.66	0.18	0.859
	S2-Con	-11.03	5.19	-2.13	0.041 ‡	-15.00	5.86	-2.56	0.015 ‡
	S3-Con	7.97	7.26	1.10	0.280	6.08	6.75	0.90	0.374
Midbrain	Con	143.21	3.15			139.96	3.22		
	S1-Con	3.91	7.09	0.55	0.585	2.38	7.16	0.33	0.742
	S2-Con	-11.34	4.91	-2.31	0.027	-12.42	4.01	-3.09	0.004 ‡
	S3-Con	-0.73	5.83	-0.13	0.901	-6.72	5.56	-1.21	0.235
Pons	Con	115.15	2.65			107.65	2.89		
	S1-Con	7.99	5.99	1.34	0.191	4.59	6.26	0.73	0.469
	S2-Con	-4.89	4.11	-1.19	0.243	-5.43	4.51	-1.20	0.237
	S3-Con	2.71	5.85	0.46	0.646	-0.98	4.95	-0.20	0.845

*Baseline nrCBF is normalized regional cerebral bloodflow measured by HMPAO-SPECT

†S1=symptom complex 1, S2=symptom complex 2, S3=symptom complex 3, and Con=controls.

‡The difference was borderline nonsignificant in the component blocks of this structure but significant for the structure as a whole (i.e., a structure-wide effect).

§Although the difference in this deep brain structure was not significant, the difference in one of the component blocks of this structure was significant (i.e., a localized block effect)

Supplementary Table S2. Physostigmine effect* in the control group and difference in the physostigmine effect between symptom complex groups and the control group at the deep brain structure level

	Effect†	Left				Right			
		mean	std err	t	p	mean	std err	t	p
Amygdala	Con	-6.55	3.38	-1.94	0.061	4.14	3.63	1.14	0.263
	S1-Con	1.24	6.88	0.18	0.858	-11.37	7.88	-1.44	0.158
	S2-Con	11.27	4.77	2.36	0.024	-9.43	5.66	-1.67	0.105 §
	S3-Con	-8.42	6.03	-1.40	0.172	-17.52	6.84	-2.56	0.015
Caudate head	Con	-4.93	2.23	-2.21	0.034	-5.00	2.53	-1.98	0.056
	S1-Con	-1.79	5.25	-0.34	0.735	0.98	5.81	0.17	0.868
	S2-Con	10.52	3.11	3.38	0.002	4.90	3.80	1.29	0.206
	S3-Con	-5.02	4.11	-1.22	0.231	1.44	5.71	0.25	0.802
Putamen	Con	-0.77	3.18	-0.24	0.809	-1.90	2.69	-0.70	0.486
	S1-Con	-0.86	6.85	-0.13	0.901	-8.77	6.25	-1.40	0.170 §
	S2-Con	6.81	5.09	1.34	0.190	5.27	4.11	1.28	0.209
	S3-Con	-4.57	6.05	-0.76	0.455	-6.40	5.13	-1.25	0.221
Globus pallidus	Con	-6.38	3.08	-2.07	0.046	3.01	2.90	1.04	0.307
	S1-Con	2.52	6.54	0.38	0.703	-7.44	7.25	-1.03	0.312
	S2-Con	11.01	4.74	2.33	0.026 ‡	1.50	5.69	0.26	0.794
	S3-Con	6.60	5.99	1.10	0.278	-6.35	7.05	-0.90	0.374
Thalamus	Con	1.05	3.15	0.34	0.739	0.81	3.33	0.24	0.810
	S1-Con	-13.10	4.73	-2.77	0.009	-1.04	7.59	-0.14	0.891
	S2-Con	7.49	5.09	1.47	0.151	7.69	4.62	1.67	0.105
	S3-Con	-12.08	7.00	-1.73	0.093	-4.25	5.29	-0.80	0.426
Hippocampus	Con	-1.42	2.58	-0.55	0.585	-2.55	3.37	-0.76	0.454
	S1-Con	3.14	4.87	0.64	0.523	-5.75	8.47	-0.68	0.502
	S2-Con	2.00	3.98	0.50	0.619	10.63	5.66	1.88	0.069 §
	S3-Con	-3.14	4.09	-0.77	0.447	4.53	7.20	0.63	0.533
Midbrain	Con	-1.57	2.84	-0.55	0.584	-2.14	3.32	-0.64	0.524
	S1-Con	-0.04	6.69	-0.01	0.996	-1.99	6.08	-0.33	0.745
	S2-Con	6.66	5.02	1.33	0.194	6.80	4.51	1.51	0.141
	S3-Con	-3.69	7.35	-0.50	0.619	-1.95	6.61	-0.29	0.770
Pons	Con	1.51	2.34	0.65	0.523	1.71	1.88	0.91	0.368
	S1-Con	-3.40	5.89	-0.58	0.567	-0.11	3.32	-0.03	0.973
	S2-Con	1.61	3.77	0.43	0.672	2.76	2.79	0.99	0.329
	S3-Con	4.82	5.49	0.88	0.386	4.04	3.97	1.02	0.316

*Physostigmine effect is the change in nrCBF from baseline to physostigmine-stimulated SPECT scan.

†S1=symptom complex 1, S2=symptom complex 2, S3=symptom complex 3, and Con=controls.

‡The difference was borderline nonsignificant in the component blocks of this structure but significant for the structure as a whole (i.e., a structure-wide effect).

§Although the difference in this deep brain structure was not significant, the difference in one of the component blocks of this structure was significant (i.e., a localized block effect)

Supplementary Table S3. Comparison of groups on demographic and study characteristics

Characteristic	Group1 (N=5)		Group2 (N=11)		Group3 (N=5)		Controls (N=17)	
	Mean	Std	Mean	Std	Mean	Std	Mean	Std
Age (yr, mean)	38.85	7.61	52.93	6.30	53.08	6.64	50.48	6.71
Lefthanded (%)	0.00	0.00	9.09	0.75	20.00	3.20	5.88	0.33
Height (cm, mean)	180.69	6.32	176.08	4.65	181.10	5.48	175.85	4.33
Weight (Kg, mean)	99.53	8.09	87.27	12.37	89.08	20.48	83.59	11.68
BMI (mean)	30.52	2.52	28.09	3.27	27.04	5.42	27.07	4.00
Daytime heart rate (BPM, mean)	85.33	6.38	80.22	7.38	86.81	7.92	82.28	8.34
daytime mean arterial BP (mmHg, mean)	95.46	3.99	100.52	6.39	98.44	3.71	96.91	8.12
Any underlying medical condition (%)	40.00	4.80	36.36	2.10	80.00	3.20	23.53	1.06
SCID diagnosis of alcohol abuse* (%)	40.00	4.80	0.00	0.00	0.00	0.00	17.65	0.85
SCID diagnosis of PTSD (%)	20.00	3.20	18.18	1.35	0.00	0.00	0.00	0.00
Smoker (%)	20.00	3.20	81.82	1.35	60.00	4.80	64.71	1.34
Fasting glucose concentration (mg/dL, mean)	104.60	12.32	97.55	14.94	103.60	7.50	102.71	12.89
Creatine clearance (ml/min, mean)	119.58	11.15	134.32	31.14	113.55	32.44	123.29	16.74
Prescription medication before study (%)	60.00	4.80	63.64	2.10	40.00	4.80	35.29	1.34
Continued prescription medicine during study (%)	40.00	4.80	63.64	2.10	40.00	4.80	17.65	0.85
Serum cholinesterase activity (U/ml, mean)	1.44	0.25	1.34	0.36	1.23	0.26	1.32	0.20
HMPAO tracer dose given at session 1 (MiC, mean)	20.84	0.67	20.72	1.61	21.46	1.84	21.07	1.88
Interval from HMPAO injection to SPECT scan (min, mean)	95.80	14.70	95.18	11.11	90.00	0.00	86.76	22.36
Physostigmine dose administered (mg, mean)	1.25	0.00	1.50	0.43	1.30	0.11	1.44	0.34
Nausea or vomiting after physostigmine (%)	80.00	3.20	54.55	2.25	80.00	3.20	64.71	1.34

*None had a diagnosis of alcohol dependence.

Supplementary Table S4A

Tests for confounding by individual covariates in the mixed-effects model* of baseline nrCBF (session1)

Covariate in single covariate model	Covariate <i>P</i>	Model statistics		Contrast syn2 vs controls		
		Group <i>P</i>	Interaction <i>P</i>	Adj Difference	StdErr	<i>P</i>
None	--	0.0070	0.0904	11.21	3.70	0.0046
Age	0.5720	0.0090	0.1080	11.56	3.78	0.0044
Lefthanded	0.0250	0.0029	0.0840	11.63	3.48	0.0021
Height	0.7380	0.0124	0.1370	11.24	3.75	0.0051
Weight	0.9080	0.0090	0.0580	11.27	3.78	0.0054
Body mass index	0.9610	0.0083	0.0560	11.19	3.78	0.0056
Daytime heart rate	0.2530	0.0045	0.0780	11.71	3.70	0.0034
Daytime mean arterial blood pressure	0.4020	0.0060	0.0790	11.95	3.81	0.0036
Any underlying medical condition	0.3790	0.0065	0.0410	10.82	3.74	0.0067
SCID diagnosis of alcohol abuse	0.8350	0.0138	0.1510	11.03	3.86	0.0073
SCID diagnosis of PTSD	0.5900	0.0073	0.0680	11.83	3.90	0.0047
Smoker	0.0250	0.0320	0.0510	9.90	3.52	0.0082
Fasting blood glucose concentration	0.3590	0.0056	0.0590	11.82	3.76	0.0035
Creatine clearance	0.9420	0.0111	0.1300	11.27	3.83	0.0060
Prescription medications before study	0.5860	0.0109	0.1330	10.71	3.85	0.0089
Continued prescription medicine during study	0.1360	0.0029	0.0770	13.63	3.96	0.0016
HMPAO tracer dose at session 1	0.9710	0.0087	0.0930	11.20	3.77	0.0055
Interval from HMPAO injection to SPECT scan	0.3180	0.0057	0.0850	12.02	3.78	0.0032

*Each mixed-effects model contained group, structure, group x structure, covariate and covariate x structure, with subject as a random effect and structure as a repeated measure.

P values highlighted in red correspond to the main findings in the global hypothesis test described in **Fig. 2A** of the paper.

Supplementary Table 4B

Test of confounding by multiple covariates* in the mixed effects model† of baseline nrCBF (session1)

Terms in multi-covariate model	<i>P</i>
Smoker	0.0162
Smoker x Structure	0.3436
Lefthanded	0.0177
Lefthanded x Structure	0.0161
SCID diagnosis of alcohol abuse	0.4897
SCID diagnosis of alcohol abuse x Structure	0.0966
Group	0.0369
Structure	<0.0001
Group x Structure	0.1361
Contrasts	
S1 vs Controls	0.7609
S2 vs Controls	0.0075
S3 vs Controls	0.9699
S1 vs S2	0.0443
S1 vs S3	0.8313
S2 vs S3	0.0400

*Structure-specific multiple regression analyses of baseline rCBF were used to identify the subset of covariates that provided the highest adjusted model R² values across all 16 deep brain structures.

†The mixed-effects model contained group, structure, group x structure, covariates and covariates x structure, with subject as a random effect and structure as a repeated measure.

P values highlighted in red correspond to the main findings in the global hypothesis test described in **Fig. 2A** of the paper.

Supplementary Table S5A

Tests for confounding in the mixed-effects model of change in nrCBF (session2 - session1)

Covariate*	Covariate <i>P</i>	Model statistics		Contrast syn2 vs controls		
		Group <i>P</i>	Interaction <i>P</i>	Adj Difference	StdErr	<i>P</i>
None	--	0.1139	0.0052	-5.59	3.09	0.0791
Age	0.4080	0.0909	0.0007	-6.01	3.14	0.0647
Lefthanded	0.0680	0.0916	0.0032	-5.87	2.98	0.0575
Height	0.4570	0.0962	0.0248	-5.54	3.11	0.0842
Weight	0.5100	0.1404	0.0017	-5.85	3.14	0.0714
Body mass index	0.3350	0.1160	0.0028	-5.94	3.11	0.0650
Daytime heart rate	0.2140	0.0680	0.0012	-6.04	3.08	0.0586
Daytime mean arterial blood pressure	0.7100	0.1176	0.0050	-5.86	3.21	0.0773
Any underlying medical condition	0.8310	0.1214	0.0108	-5.50	3.16	0.0904
SCID diagnosis of alcohol abuse	0.8120	0.1531	0.0137	-5.41	3.22	0.1026
SCID diagnosis of PTSD	0.5590	0.1064	0.0032	-6.14	3.26	0.0683
Smoker	0.9130	0.1610	0.0073	-5.53	3.18	0.0909
Fasting blood glucose concentration	0.1690	0.0676	0.0047	-6.34	3.09	0.0483
Creatine clearance	0.6420	0.1151	0.0076	-5.89	3.19	0.0739
Prescription medications before study	0.7580	0.1400	0.0112	-5.35	3.22	0.1068
Prescription medicine continued during study	0.9700	0.1415	0.0059	-5.64	3.42	0.1089
Serum butyryl-cholinesterase activity	0.9440	0.1237	0.0071	-5.58	3.14	0.0846
Dose of physostigmine administered	0.0450	0.0381	0.0118	-6.07	2.96	0.0481
Difference in HMPAO dose at sessions 1 and 2	0.3880	0.1375	0.0055	-5.03	3.16	0.1215
Difference in interval from HMPAO injection to scan	0.8640	0.1351	0.0202	-5.82	3.42	0.0985
Nausea or vomiting in response to physostigmine	0.1738	0.0703	0.0062	-5.97	3.06	0.0594

*Each mixed-effects model contained group, structure, group x structure, covariate and covariate x structure, with subject as a random effect and structure as a repeated measure.

P values highlighted in red correspond to the main finding in the global hypothesis test described in **Fig. 2B** of the paper.

Supplementary Table S5B

Test of confounding by multiple covariates* in the mixed effects model† of change in nrCBF (session2 - session1)

Terms in multi-covariate model	<i>P</i>
Lefthanded	0.1100
Lefthanded x Structure	0.2600
Daytime mean arterial blood pressure	0.7953
Daytime mean arterial blood pressure x Structure	0.1325
Body mass index	0.5806
Body mass index x Structure	0.5130
Group	0.1440
Structure	0.0218
Group x Structure	0.0031
Contrasts	
S1 vs Controls	0.5489
S2 vs Controls	0.0717
S3 vs Controls	0.6256
S1 vs S2	0.0716
S1 vs S3	0.9155
S2 vs S3	0.0801

*Structure-specific multiple regression analyses of baseline rCBF were used to identify the subset of covariates that provided the highest adjusted model R^2 values across all 16 deep brain structures.

†The mixed-effects model contained group, structure, group x structure, covariates and covariates x structure, with subject as a random effect and structure as a repeated measure.

P values highlighted in red correspond to the main finding in the global hypothesis test described in **Fig. 2B** of the paper.

Supplementary Table S6
Controlling for physostigmine dose in the model
of change in nrCBF (session2 - session 1)

Effect	P value	
	Model 1	Model 2
Group	0.115	0.038
Physostigmine dose	–	0.045
Structure	0.002	0.002
Group by Structure	0.005	0.005
Contrast:		
Control vs S1	0.485	0.269
Control vs S2	0.079	0.048
Control vs S3	0.446	0.281
S2 vs S1	0.058	0.018
S2 vs S3	0.051	0.019
S1 vs S3	0.959	0.975

Model 1 is the original global hypothesis test, the estimates from which are shown in **Fig. 1B** of the paper. Model 2 is the same analysis but controlling for physostigmine dose.